J Nanopart Res (2020) 22: 167
https://doi.org/10.1007/s11051-020-04903-w

RESEARCH PAPER

Sodium hexametaphosphate–induced enhancement of silver nanoparticle toxicity towards leukemia cells

Magdalena Oćwieja · **Anna Barbasz**

Received: 13 January 2020 / Accepted: 2 June 2020 / Published online: 15 June 2020

Abstract Synergistic effects occurring between biologically active substances are of great importance for efficient treatment of many diseases. Therefore, the aim of research was to determine impact of sodium hexametaphosphate (HEX), which is a well-known permeabilizer, on the cytotoxicity of silver ions and two types of AgNPs towards HL-60 and U-937 tumor cells. The AgNPs were synthesized in a chemical reduction method using sodium borohydride and trisodium citrate (CITAgNPS) or sodium hypophosphite and HEX (HEXAgNPs). Imaging with the use of transmission electron microscopy (TEM) and atomic force microscopy (AFM) revealed that the AgNPs exhibited spherical shape and comparable size distribution. Electrophoretic mobility studies showed that the AgNPs were negatively charged. The mitochondrial and antioxidant activity as well as membrane lipid peroxidation and integrity after dose-dependent AgNP treatment were evaluated using biochemical assays. The impact of HEXAgNPs on the membrane integrity and inactivation of antioxidant enzymes of the cells was much higher than this one observed for CITAgNPs and silver ions of the same concentration. The membrane damage occurred as a result of lipid peroxidation which was induced by pure HEX and HEXAgNPs. It was also observed that HEX significantly increased cell membrane damage induced by CITAgNPs and silver ions although the cells exhibited different sensitivity to these components. Moreover, it was found that HEX can induce oxidative stress. Hence, it was revealed that HEX enhances AgNP activity when it is applied both as their stabilizer or supplement in their suspensions.

Keywords Silver nanoparticles · Tumor cells · Permeabilizers · Cytotoxicity · Enhancement effects · Sodium hexametaphosphate · Health effects

Introduction

Numerous literature reports describing research with living organisms have indicated that biological activity of silver nanoparticles (AgNPs) strongly depends on their size (Carlson et al. 2008; Lu et al. 2013), morphology (Pal et al. 2007), and surface properties including surface charge (Fröhlich 2012; Jiang et al. 2009; Suresh

Electronic supplementary material The online version of this article (https://doi.org/10.1007/s11051-020-04903-w) contains supplementary material, which is available to authorized users.

M. Oćwieja (✉)
Jerzy Haber Institute of Catalysis and Surface Chemistry, Polish Academy of Sciences, Niezapominajek 8, PL-30239 Krakow, Poland

A. Barbasz
Institute of Biology, Pedagogical University, Podchorążych 2, 30-084 Krakow, Poland

et al. 2012) and chemical structure of stabilizing layer (Ahamed et al. 2008; Kujda et al. 2015). First of all, it was found that AgNPs smaller than 20 nm exhibit the highest biological activity because they can be transported by the cell membrane via endocytosis in both eukaryotic and prokaryotic cells (Ding and Ma 2012; Zhang et al. 2009). Based on the results of experimental studies, it was documented that some positively charged AgNPs are more toxic towards numerous pathogens and cancer cells than negatively charged nanoparticles (Abbaszadegan et al. 2015; Suresh et al. 2012). This effect was mainly explained by the attractive electrostatic interactions which occur between AgNPs and negatively charged cell membranes. Thanks to them, the penetration of AgNPs to cells and their intracellular action are significantly facilitated. Nevertheless, the surface charge of AgNPs is mainly tuned by molecules of stabilizing agents adsorbed on their surface (Abbaszadegan et al. 2015; Le Ouay and Stellacci 2015). Therefore, the presence of these molecules also plays a pivotal role in the bioactivity of AgNPs (Pokhrel et al. 2013).

Recently, the research on synergistic effects between AgNPs and biologically active molecules has been in the center of attention of scientists dealing with nanomaterials and biological systems. Among various examples of such research, one should mention about these ones which were focused on the synergy of AgNPs with antibiotics (Fayaz et al. 2010; Hwang et al. 2012; Li et al. 2005). For instance, conducted studies proved that antibacterial activity of ampicillin, kanamycin, erythromycin, and chloramphenicol against gram-positive and gram-negative bacteria was enhanced in the presence of AgNPs. The proposed mechanism of the action of the AgNPs-antibiotic conjugates assumed that the antibiotics acting on the cell walls of bacteria caused their lysis which increased the penetration of AgNPs to the cells of bacterium (Hwang et al. 2012).

Enhanced biological activity towards gram-negative bacteria was also documented in the case of various combinations of silver ions and AgNPs with some antimicrobial peptides (AMPs) increasing the permeability of biological membranes (Ruden et al. 2009).

Synergistic effects were also observed in the case of combinations of silver ions and AgNPs (Huang et al. 2011; Potara et al. 2011) with chitosan which exhibits antibacterial, anti-inflammatory and analgesic properties (Cao 2017; Kumar-Krishnan et al. 2015). It was established that in such combinations, chitosan destabilizes outer membranes of bacteria, decreasing their integrity and allowing AgNPs to easily penetrate the interior of the microbial cells where they carry out their killing action (Cao 2017; Huang et al. 2011).

Sodium hexametaphosphate (HEX) is another well-known inorganic permeabilizer which can act as a nanoparticle stabilizing agent (Vaara 1992; Vaara and Jaakkola 1989). It was documented that this polyphosphate can stabilize such nanoparticles as zinc sulfide (Warad et al. 2005), barium sulfate (Gupta et al. 2010), as well as gold nanoparticles (AuNPs) (Parab et al. 2011) and AgNPs (Li et al. 2010; Liu et al. 2010) in the presence of polyvinyl pyrrolidone (PVP). HEX belongs to food-grade permeabilizers and it is widely used as a sequestering agent, a curing agent, emulsifier, corrosion inhibitor, surface-active agent, synergistic, and texturizer (Lanigan 2001), to name a few of its applications. It is worth mentioning that due to unique physicochemical properties (Lanigan 2001; Post et al. 1963), HEX is used in cosmetics and dental products (Bae et al. 2015; Dalpasquale et al. 2017). The oral toxicity of HEX is estimated at 3053 mg kg^{-1} (Parab et al. 2011). It was noticed that HEX extensively hydrolyzes to orthophosphate in rats and rabbits after intravenous (IV), intraperitoneal (IP), and subcutaneous administration (Lanigan 2001). Then, it was established that HEX was poisonous by the IV route, moderately toxic by IP and subcutaneous routes, and mildly toxic by ingestion. Furthermore, one of the latest research revealed that HEX can stimulate growth, differentiation, and angiogenic potential of human dental pulp cells (HDPCs) which makes it a promising candidate for dental pulp tissue engineering and regenerative endodontic (Bae et al. 2015).

Although HEX is not usually regarded as an antimicrobial agent (Vaara and Jaakkola 1989), some literature evidences documented that it inhibits the growth and proliferation of phatogenic bacteria. The studies conducted by Post et al. (1963) showed that in the case of gram-positive and gram-negative bacteria, HEX interferes with divalent cation metabolism causing cell division. On the other hand, Vaara and Jaakkola proved (1989) that HEX can be exploited as an excellent sensitizer in antimicrobial combinations. Subsequent studies revealed also that the combination of HEX with silver ions (Humphreys et al. 2011) and AgNPs (Kujda et al. 2015; Mendes-Gouvêa et al. 2018) enhances their toxicity towards pathogenic fungi and bacteria.

Mendes-Gouvêa et al. (2018) studied the efficiency of nanocomposites formed by mixing AgNPs, silver ions, polyphosphate, and ammonium salt of polymethacrylic acid in the deactivation of dental caries pathogens. It was observed that HEX improved antimicrobial activity of silver which enables to use a smaller amount of AgNPs to produce more biocompatible materials dedicated to application in dentistry (Mendes-Gouvêa et al. 2018). Similarly, Kujda et al. (2015) demonstrated that the concentration of HEX-stabilized AgNPs, which totally deactivates tetracycline-resistant strains of *E. coli*, wasmuch lower than in the case of other negatively charged AgNPs of comparable size distribution.

Taking into account wide range of application of HEX as well as AgNPs and considering above mentioned evidence describing the increased bactericidal activity of their compositions, our current studies were oriented towards determination of the impact of HEX on the toxicity of silver ions and AgNPs towards human histiocytic lymphoma cells (U-937) and human promyelocytic cells (HL-60). In contrast to previous studies devoted to bactericidal effects, in this report the attention was focused on the properties of Ag-HEX compositions. It was hypothesized that the presence of HEX can enhance the biological activity of AgNPs. Conducted research included an assessment of toxicity of three various compositions of silver, namely AgNPs stabilized by HEX as well as mixtures of HEX with citrate-stabilized AgNPs (CITAgNPs) and silver ions delivered in the form of silver nitrate.

Materials

Chemicals and materials

Silver nitrate ($AgNO_3$), sodium hypophosphite (HPH), sodium hexametaphosphate (HEX), sodium borohydride, sodium chloride, and trisodium citrate dehydrate (CIT) were commercial products of Sigma-Aldrich. Sulfuric acid, sodium hydroxide, and hydrochloric acid were obtained from Avantor Performance Materials Poland S.A. (formerly POCH S.A., Gliwice, Poland). All reagents were used without further purification. Ultrapure water (conductivity 0.06 μS cm^{-1}), applied for preparation of all solutions and the synthesis of silver nanoparticles, was obtained from the Milli-Q Elix & Simplicity 185 purification system (Millipore SA Molsheim, France).

AgNPs stabilized by sodium hexametaphosphate, indicated as HEXAgNPs, were obtained by a chemical reduction method according to the procedure developed previously (Adamczyk et al. 2016; Kujda et al. 2015). Briefly, 30 mg of sodium hexametaphosphate and 445 mg of sodium hypophosphite were dissolved in 160 mL of 1 mM solution of sulfuric acid. Then, this solution was heated to 40 °C and mixed with 50 mL solution of silver nitrate of concentration 10 mM. At this temperature, the reaction mixture was stirred over 1 h. After this period of time, obtained silver nanoparticle suspension was purified from unreacted compounds using the ultrafiltration method (Kujda et al. 2015). For this purpose, the Amicon 8400 ultrafiltration cell equipped with a polyethersulfone membrane (Millipore, PBHK07610) was used.

Silver nanoparticles stabilized by citrate anions, described as CITAgNPs, were synthesized via reduction of silver ions by sodium borohydride in the presence of trisodium citrate. The synthesis details were widely described in previous work (Kujda et al. 2015).

Cell lines

Histiocytic lymphoma (U-937) and human promyelocytic (HL-60) cell lines were purchase from American Type Culture Collection (ATCC). The cells were growth in RPMI 160 medium supplemented with 5–10% fetal bovine serum (FBS) and 0.01% penicillin-streptomycin at 37 °C in a humidified atmosphere (Barbasz et al. 2017). The culture medium, FBS, and antibiotics were obtained from CytoGEn GmbH.

Methods

Characteristics of AgNPs

Mass concentration of the nanoparticles in the stock suspensions was determined from the measurements of the density of these suspensions and effluents obtained during the purification procedure. For this purpose, the DMA5000M densitometer from Anton Paar company and the procedure developed previously were applied (Kujda et al. 2015). Additionally, the AgNP concentration in the suspensions and the amount of leached silver ions in the effluents were measured using ionmeter SevenCompact S220B equipped with Ag^{+}/S^{2-} ion-

selective electrode and a PinAAcle 900Z atomic absorption spectrometer (Perkin Elmer).

UV-vis spectra of the nanoparticle dispersed in the stock suspensions and culture media were recorded using Shimadzu UV-1800 spectrometer. pH and electric conductivity of the suspensions were measured with the use of the CPC-505 apparatus connected with electrode ERH-12-6 and conductometric sensor EC-201t.

The morphology of AgNPs was investigated by means of transmission electron microscopy (TEM) using the FEI Tecnai G2 microscope at 200 kV equipped with high-angle annular dark-field scanning transmission HAADF/STEM and EDAX energy dispersive X-ray (EDX) detectors. Additionally, the JEOL JSM-7500F microscope working in a transmission mode was applied. The AgNPs were also investigated using NT-MDT Solver PRO atomic force microscopy (AFM) equipped with the SMENA SFC050L scanning head. In the first case, the drop of the stock suspension was placed on a copper grid covered by carbon film and after the evaporation of water, the AgNPs were imaged in a dark and bright field. In the case of AFM studies, the nanoparticles were deposited on freshly cleaved mica sheets (Continental Trade Ltd.) coverd by poly (allylaminehydrochloride)(PAH) (Morga and Adamczyk 2013) under diffusion transport conditions. The deposition process was carried out using the stock suspension whereas the time of nanoparticle deposition was equal to 2 h. The morphology and size distribution of nanoparticles were analyzed with the use of MultiScan software (Computer Scanning System).

Zetasizer Nano ZS (Malvern) apparatus was applied in order to measure the diffusion coefficients and electrophoretic mobility of the nanoparticles dispersed in the suspensions of controlled ionic strength and pH. From these measurements, the nanoparticle hydrodynamic diameter and zeta potential were calculated using the Stokes-Einstein and the Henry equations, respectively (Kujda et al. 2015). The number of uncompensated charges (N_c) on the nanoparticles was determined from the Lorentz-Stokes relationship (Morga and Adamczyk 2013). Moreover, 2D electrokinetic charge densities (σ_e) were estimated from the relationship described elsewhere (Morga and Adamczyk 2013).

Cell viability

In typical experiments, the cells, in a volume of 0.2 mL and in an amount of 1×10^6 cells per mL, were seeded in 96-well and they were incubated with various concentrations of the silver nanoparticles (from 0 to 60 mg L^{-1}). The plates with the cells were incubated over 24 h at 37 °C. After this period of time, the samples were collected, centrifuged (1000×*g*, 5 min) and analyzed. In additional experiments, the cells were incubated with silver nitrate ($AgNO_3$), sodium hexametaphosphate (HEX), sodium hypophosphite (HPH) and with the mixtures of the AgNPs or $AgNO_3$ with HEX of various concentrations.

Lactate dehydrogenase leakage (LDH assay) and 3-(4,5-dimethylthiazol-2-yl)-2,5-diphenyl tetrazolium bromide) reduction (MTT assay) were used for determination of the cell viability (Barbasz et al. 2017) after the silver and phosphate treatments (in each case the incubation time was 24 h). In the first case, 100 μL of the supernatants obtained after the centrifugation was added to the mixture of 0.5 mL 0.75 mM sodium pyruvate and 10 μL of 140 μM NADH. Such mixtures were incubated at a temperature of 37 °C for over 30 min. Afterwards, 0.5 mL of 0.1 M of 2,4-dinitrophenylhydrazine was added to each of the mixtures. After 1 h of addition, the absorbance of formed hydrazone was measured at 450 nm using the microplate reader Epoch (BioTek Instruments). Final value of absorbance was calculated taking into account the contribution to the absorbance value from blank reagent. The release of LDH from the nanoparticle-treated cells was calculated compared to the control in which the release of LDH was equal 100% due to disruptions of membranes in the cells via sonification.

The MTT assay was assessed by adding 50 μL MTT of concentration equal to 5 mg L^{-1} to each well containing the cells treated by the AgNPs. Such mixtures were left at 37 °C over 2 h and then they were supplemented by 0.4 mL of dimethyl sulfoxide (DMSO). After 5 min of the addition, the mixtures were centrifuged and the absorbance of supernatants was measured at 570 nm using the aforementioned microplate reader. It is worth mentioning that value of measured absorbance corresponded to the number of viable cells. Therefore, having this value and knowing absorbance of a sample containing the same number of living cells, the viability of the cells after the AgNP treatment was calculated.

Membrane lipid peroxidation

Membrane lipid peroxidation was evaluated spectrophotometrically measuring absorbance of thiobarbituric

acid and malondialdehyde (MDA) complex at 532 nm. For this purpose, 0.5 mL of 0.5% trichloroacetic acid (TCA) was added to obtained supernatants. Then, the mixtures were vortexed for 1 min and lysed over 5 min using ultrasonic bath (15 kHz). The samples were centrifuged (10 min, 10,000×*g*) and finally added to 1.25 mL of a solution of 20% TCA and 0.5% TBA. After 30 min of heating at 100 °C, the samples were cooled to ambient temperature and characterized spectrophotometrically. The concentration of MDA was determined using the value of measured absorbance at $\lambda =$ 532 nm and knowing the value of molar extinction coefficient of MDA which is equal to 155 mM^{-1} cm^{-1}.

Superoxide dismutase activity

After the nanoparticle treatment, centrifuged cells were vortexed in 0.05 M phosphate buffer solution of pH 7.2 containing 0.1% BSA and 0.1 mM EDTA. Then, they were sonicated at 15 kHz over 5 min. After the centrifugation (10,000×*g*, 5 min), the concentration of SOD in the supernatants was determined spectrophotometrically. For this purpose, the supernatant solution and xanthine oxidase were added to the mixture of 0.05 M phosphate buffer (pH 7.2), 0.1 mM EDTA, 0.1 mM cytochrome C and 0.1 mM solution of xanthine of individually selected volume ration. For each sample absorbance was measured at a wavelength of 550 nm after 2 min of the mixing. It was assumed that at ambient temperature one unit of activity (1 U) corresponds with such concentration of enzyme which caused the cytochrome C inhibiton by 50%. The SOD activity was expressed relative to the protein content in the supernatants.

Statistical analysis

All values were calculated from three independent experiments and presented in the graphs as the mean and standard deviation (SD). The statistical analysis was performed by Duncan's multiple range test, taking $p < 0.05$ using PC SAS 8.0 software (SAS Institute, NC).

Results

Characteristics of AgNPs and their suspensions

HEXAgNPs were obtained by the reduction of silver ions with sodium hypophosphite at acidic medium which is needed for the transformation of the inactive form of phosphate to an active one (Li et al. 2010) (Supporting materials). The process was carried out at an elevated temperature in the presence of HEX which is a poor reducing agent and it plays the role of a stabilizer. It is worth mentioning that in the previous literature reports describing the preparation of AgNPs (Li et al. 2010; Liu et al. 2010) or AuNPs capped by HEX, the PVP was additionally used to improve the stability of the nanoparticles. HEXAgNPs investigated in this work were prepared according to the developed synthesis method which eliminates the addition of PVP (Adamczyk et al. 2016; Kujda et al. 2015).

CITAgNPs were prepared according to the well-known method relies on a reduction of silver ions in the medium containing sodium borohydride and trisodium citrate (Barbasz et al. 2017). It is worth mentioning that trisodium citrate, used as a capping agent of CITAgNPs, is a derivative of citric acid which in turn is less common food-grade permeabilizer (Helander and Mattila-Sandholm 2000). Hence, both types of AgNPs used in these studies were stabilized by potentially non-toxic substances, widely applied in food processing.

In the beginning, the formation of AgNPs was confirmed by measurements of extinction spectra of their suspensions (supporting materials, Fig. 2S). The maximum absorption bands appeared at a wavelength of 400 nm and 394 nm for the suspension of HEXAgNPs and CITAgNPs, respectively.

The suspensions were carefully filtrated until the conductivity of the effluents reached a value of 15 μS cm^{-1}, and pH was stabilized on the same level of 5.6. It was determined that the mass concentration of the AgNPs in the stock suspensions was equal to 64 and 81 mg L^{-1} in the case of HEXAgNPs and CITAgNPs, respectively (Table 1). The concentration of free silver ions, determined by AAS and ion-selective electrode, in the freshly purified suspensions was lower than the limit detection of these methods. After 30 days of storage of the suspensions, the concentration of leached silver ions increased to a value of 0.48 ± 0.05 and 0.63 ± 0.01 mg L^{-1} for HEXAgNPs and CITAgNPs, respectively. Comparing these values with other literature data including determination of silver ions release form AgNPs (Guo et al. 2013; Kaba et al. 2015; Kittler et al. 2010; Li et al. 2013, Zhang et al. 2011), one can state that under-investigated conditions (Table 1) these nanoparticles were rather resistant to oxidative dissolution.

Recorded TEM micrographs (Fig. 1) and AFM images (Supporting materials, Fig. 3S) revealed that the nanoparticles were spherical in shape. Moreover, they were characterized by comparable size distribution. The average size of HEXAgNPs was equal to 14 ± 4 nm whereas CITAgNPs were slightly smaller of an average size of 12 ± 6 nm and higher polydispersity index (Table 1).

Based on the diffusion coefficients of the AgNPs, which were measured under controlled conditions of pH and ionic strength with the use of the DLS technique (Kujda et al. 2015), the hydrodynamic diameters were calculated and collected in Table 1. It is worth noticing that comparable values of diameters obtained for the AgNPs deposited on solid surfaces and determined under dry conditions (TEM, AFM) as well as for the nanoparticles dispersed in the suspensions (DLS) indicate on the insignificant contribution of the thickness of stabilizing layers to the total size of the nanoparticles.

The stability of the AgNPs was investigated at a broad range of pH as well as for fixed ionic strength and temperature. The results of these studies were shown in Fig. 2a as dependencies of the AgNP hydrodynamic diameter on pH. Analyzing this data one can notice that in the range of pH from 4.0 to 8.0 the hydrodynamic diameters of the AgNPs attained stable values comparable with these determined from the microscopic techniques. At pH < 4.0 the hydrodynamic diameter of CITAgNPs increased significantly indicating their aggregation. Otherwise, the instability of HEXAgNPs was observed at pH > 8.1.

The electrophoretic mobility of the AgNPs was measured under the same conditions of pH, ionic strength, and temperature as their diffusion coefficients. Then, from obtained values, the zeta potential, and other electrokinetic properties of the AgNPs were calculated and collected in Table 1. The dependencies of the nanoparticle zeta potential on pH were presented in Fig. 2b. As can be seen, both types of AgNPs exhibited negative zeta potential decreasing with pH. HEXAgNPs were less negatively charged than CITAgNPs. For instance, at pH 7.4, the zeta potential of HEXAgNPs attained a value of − 47 mV whereas in the case of CITAgNPs it was equal to − 55 mV.

Based on conducted physicochemical characteristics (Figs. 1 and 2 and Fig. 2S-5S), one can reach the general

Table 1 Properties of silver nanoparticles and their suspensions

Property/conditions	Silver nanoparticles	
Compounds used during synthesis	HEXAgNPs Sodium hypophosphite, sodium hexametaphosphate	CITAgNPs Sodium borohydride, trisodium citrate
Concentration of nanoparticles in stock suspension [mg L^{-1}]	64	81
pH of stock suspension	5.6	5.6
Absorption maximum [nm]	400	394
Diffusion coefficients [× 10^{-7} cm^2 s^{-1}] determined at 37 °C, pH 5.6 and ionic strength 10^{-2} M	4.96	5.86
Hydrodynamic diameter [nm] determined at 37 °C, pH 5.6 and ionic strength 10^{-2} M	13 ± 4	11 ± 4
Polydispersity index (PdI) determined at 37 °C, pH 5.6 and ionic strength 10^{-2} M	0.32 ± 0.05	0.34 ± 0.07
Size [nm] determined from TEM micrographs (and AFM images)	14 ± 4 (18 ± 5)	12 ± 6 (17 ± 6)
Electrophoretic mobility (μmcm $(Vs)^{-1}$) determined at 37 °C, pH 5.6 and ionic strength 10^{-2} M	−2.9 ± 0.1	−3.6 ± 0.1
Zeta potential (μmcm$(Vs)^{-1}$) determined at 37 °C, pH 5.6, and ionic strength 10^{-2} M	−45 ± 3	−54 ± 2
Number of uncompensated charges (N_c) [e] calculated for 37 °C, pH 5.6 and ionic strength 10^{-2} M	(−) 15	(−) 16
2D electrokinetic charge densities (σ_e) [e nm^{-2}] calculated for 37 °C, pH 5.6, and ionic strength 10^{-2} M NaCl	(−) 0.0282	(−) 0.0289
The concentration of leached silver ions (mg L^{-1}) determined in the effluents at a dissolved oxygen concentration of 7.8 mg L^{-1} and 25 °C after 30 days of preparation and purification	0.48 ± 0.05	0.63 ± 0.01

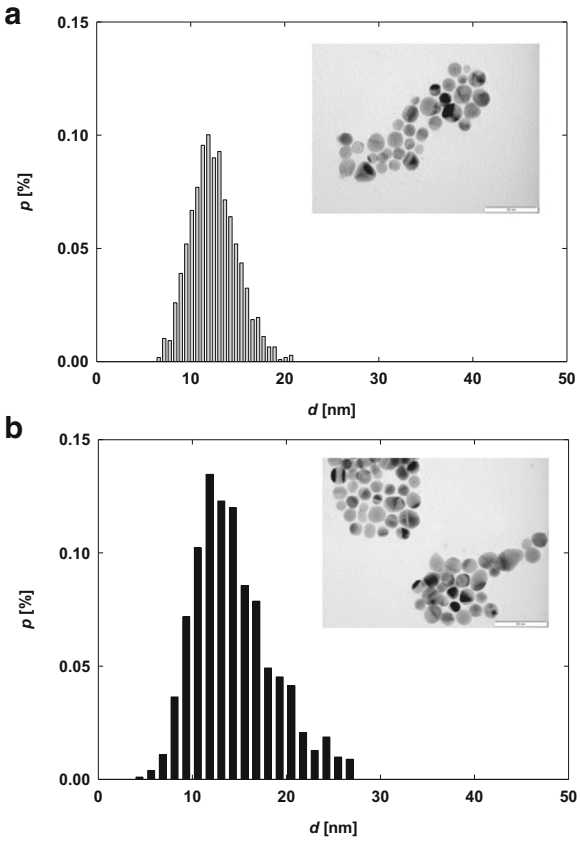

Fig. 1 Size distribution of (**a**) HEXAgNPs and (**b**) CITAgNPs and typical HRTEM micrographs (inserts) presenting the nanoparticles

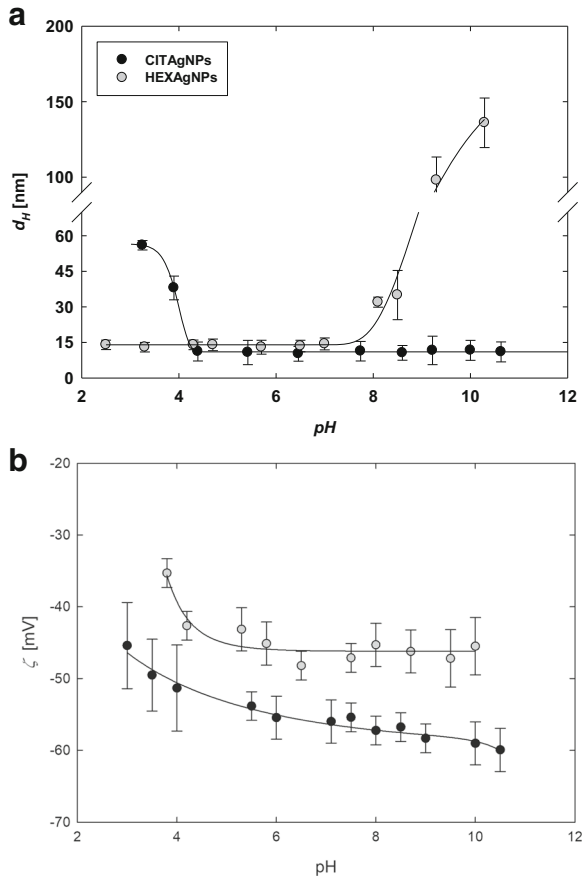

Fig. 2 Dependence of (**a**) hydrodynamic diameter and (**b**) zeta potential of HEXAgNPs (gray circle) and CITAgNPs (black circle) on pH determined at ionic strength 10^{-2} M NaCl and temperature of 37 °C. The concentration of the suspensions was equal to 50 mg L^{-1}. Solid lines present nonlinear fits of experimental results.

conclusion that prepared AgNPs were characterized by comparable morphological features, size distribution, surface charge, and ion release profile but they differed in the chemical structure of the stabilizing layer.

Cell membrane damage induced by silver ions, AgNPs, and their stabilizers

Histiocytic lymphoma (U-937) and human promyelocytic (HL-60) cell lines were selected for biological studies designed to determine the toxicity of the AgNPs. It is worth mentioning that these cells belong to the human immune system and they as the first interact with xenobiotics. Additionally, in the literature, many reports devoted to the anticancer activity of AgNPs describe the experimental studies conducted with the use of these cells (Avalos et al. 2014; Ávalos Fúnez et al. 2013; Guo et al. 2013; Kaba and Egorova 2015).

The viability of U-937 and HL-60 cells after the AgNP treatment was assessed using MTT (Supporting materials, Fig. 6S) and LDH assays. Taking into account that the stabilizers of AgNP exhibit biological activity and are able to permeabilize cell membranes, these studies were mainly oriented towards the investigation of the cell membrane damage determined via the leakage of lactate dehydrogenase (LDH). The membrane integrity was studied in the case of the cells incubated with the AgNPs, silver ions, HEX, sodium hypophosphite, and mixtures of these two phosphate salts (Supporting materials, Fig. 7S and Fig. 8S). Basic concentrations of the phosphate mixtures applied in the biological tests were similar as these applied during the synthesis of the AgNPs. Additionally, the toxicity of some diluted solutions of phosphate salts was assessed (Supporting materials, Fig. 8S).

The results of LDH assay for U-937 and HL-60 cells after 24 h of treatment with the AgNPs, silver ions, and HEX were presented in Fig. 3. Analyzing these results one can notice a significant increase of LDH leakage with an increase of each active substance. Nevertheless, comparing the LDH release for silver concentration higher than 8 mg L^{-1} one can observe that the AgNPs were more toxic than silver ions. For instance, at a concentration of 16 mg L^{-1}, the release of LDH caused by HEXAgNPs was equal to 61% and 74% for U-937 and HL-60 cells whereas for silver ions this parameter attained a value of 38% and 32% in the case of U-937 and HL-60 cells, respectively.

Comparing the cell membrane damage induced by the AgNPs one can observe that at their lower concentrations (2 and 4 mg L^{-1}), the leaching of LDH from damaged cells was comparable. Otherwise, at higher concentrations, HEXAgNPs were more toxic towards U-937 and HL-60 cells than CITAgNPs. Interestingly, U-937 cells were more sensitive to the HEXAgNP treatment at a concentration of 2 and 4 mg L^{-1}. On the other hand, the stronger membrane damage was induced in HL-60 than in U-937 cells at HEXAgNPs concentration of 8 and 16 mg L^{-1}.

The results obtained for pure solutions of HEX showed that it also reduced the viability of both cell lines (Supporting materials Fig. 6S). Nevertheless, the release of LDH induced by HEX was significantly lower than in the case of the AgNPs and silver ions. It is worth noticing that the application of the HEX concentration of 120 mg L^{-1} did not cause such a high LDH release as in the case of HEXAgNPs of concentration of 32 mg L^{-1}. Moreover, it was found that independently on the HEX concentration, HL-60 cells were much more sensitive to the treatment than U-937 cells.

Additional experiments, conducted for pure solutions of sodium hypophosphite and its mixtures with HEX, revealed also that at low concentration their influence on the cell membrane damage was minor (Supporting materials, Fig. 7S). In turn, the results gained from the MTT assay confirmed that HEXAgNPs were the most toxic of all examined systems and caused a significant decrease in the mitochondrial functions of the cells causing their death (Supporting materials, Fig. 6S).

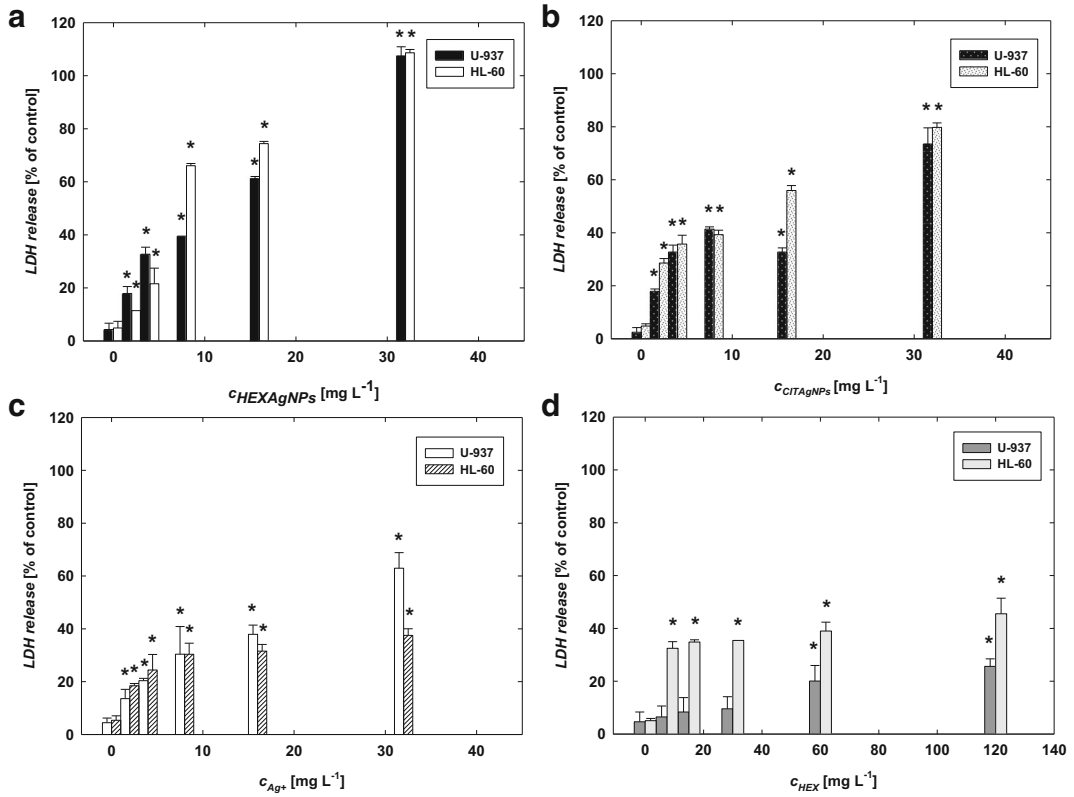

Fig. 3 Membrane damage indicated via LDH release after the cell treatment with: (**a**) HEXAgNPs, (**b**) CITAgNPs, (**c**) Ag^+ (delivered as $AgNO_3$), and (**d**) HEX. (*) Statistically significant differences ($p < 0.05$) compared to controls

Considering that the loss of cell membrane integrity, determined by LDH assay (Fig. 3), may occur as a result of membrane lipid peroxidation induced by the oxidative stress, MDA assay was introduced in the next stage of studies. The results of the research obtained for HEXAgNPs and HEX were shown in Fig. 4. Similarly, as in the case of LDH assay, it was observed that the lipid peroxidation increased with the concentration of HEXAgNPs and pure HEX. In the case of HEXAgNPs of concentration of 8 mg L^{-1}, the secretion of MDA was equal to 1.43 97 μM/2 × 10^6 cells and 1.97 μM/2 × 10^6 cells for U-937 and HL-60 cells, respectively. Otherwise, the treatment of the cells with HEX of concentration of 7.5 mg L^{-1} induced smaller MDA secretion which attained a value of 0.27 μM/2 × 10^6 cells and 0.41 μM/2 × 10^6 in the case of U-937 and HL-60 cells. Moreover, the MDA assay also showed that U-937 were less sensitive to HEX treatment than HL-60 cells. The

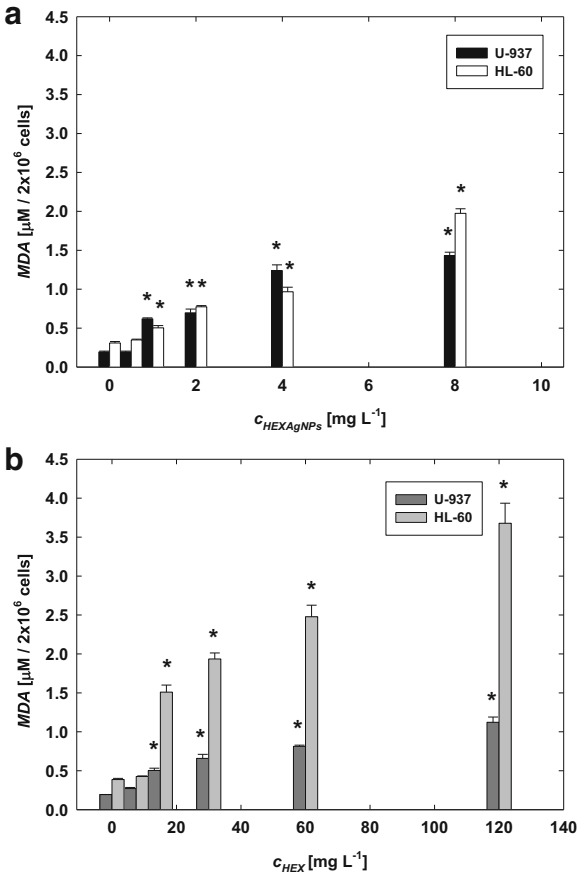

Fig. 4 Membrane lipid peroxidation determined via MDA assay for the cells after their treatment with (**a**) HEXAgNPs and (**b**) HEX. (*) Statistically significant differences ($p < 0.05$) compared to controls

oxidative stress causing lipid peroxidation and MDA secretion was the highest at the highest MDA concentration.

The lipid peroxidation in both cell lines caused by CITAgNPs and determined by MDA assay was described in detail in our previous work (Barbasz et al. 2017). Comparing these literature results with the data obtained for HEXAgNPs, one can indicate that CITAgNPs induced slightly lower membrane lipid peroxidation.

Influence of HEX on cell membrane damage induced by CITAgNPs and silver ions

In order to precisely assess the impact of HEX on the toxicity of HEXAgNPs, LDH release was determined after the treatment of the cells with a mixture of HEX with CITAgNPs or silver ions. In the first part of the studies, the cells were incubated in the suspensions of diverse mass concentration of CITAgNPs and at a constant concentration of HEX which was equal to 120 mg L^{-1}. The concentration of CITAgNPs was maintained at the same range as previously (Fig. 3b). Moreover, the LDH release was investigated after the application of the mixtures with a given concentration of CITAgNPs and of various amounts of HEX. The CITAgNP concentration of 4 mg L^{-1} was selected for the studies because as it was shown previously at this value the cell viability was attained value ca. 40% (Barbasz et al. 2017). It is noteworthy that before the biological studies the stability of CITAgNPs in the presence of HEX was confirmed via DLS and electrophoretic mobility measurements (Supporting materials, Fig. 5S).

The results of these cross-tests were presented in Fig. 5. Similarly as before (Fig. 3b), the LDH release increased with the concentration of CITAgNPs (Fig. 5a). Moreover, HL-60 cells were noticeably more sensitive to the treatment with the mixtures than U-937 cells. The LDH release from the cells treated with the mixtures of CITAgNPs and HEX was significantly higher than in the case of pure suspensions of CITAgNPs of the same concentration. At CITAgNP concentration of 8 mg L^{-1}, the LDH release attained value of ca. 40% (Fig. 3b) in the case of the pure suspension and up to 60% for the mixture with HEX (Fig. 5a).

The low concentration of HEX (7.5–30 mg L^{-1}) in the CITAgNP suspension of concentration of 4 mg L^{-1} did not enhance considerably the LDH leakage in

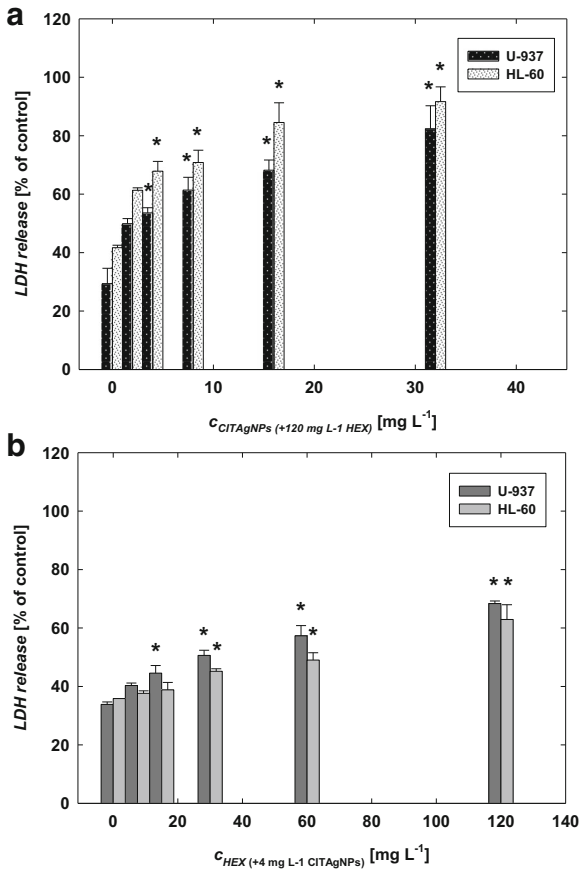

Fig. 5 Membrane damage indicated via LDH release after the cell treatment with: (**a**) CITAgNPs in the presence of HEX of concentration 120 mg L^{-1}, (**b**) HEX in the presence of CITAgNPs of concentration of 4 mg L^{-1}. (*) Statistically significant differences ($p < 0.05$) compared to controls

comparison to the pure suspension (Fig. 5b). At HEX concentration of 120 mg L^{-1}, the LDH release for both cell lines increased by ca. 20% relative to pure CITAgNPs. However, it is worth noticing that the amount of released LDH found for this mixture was lower than the total value of LDH which can be calculated adding the LDH values determined for pure CITAgNPs (Fig. 3b) and HEX (Fig. 3d) of the same concentration which was applied in the mixture (Fig. 5b).

In the second part of the cross-tests, the influence of the mixtures of HEX with silver ions delivered in the form of silver nitrate on the cell membrane damage was investigated. The measurements of LDH release were conducted in two series, namely for mixtures of a fixed concentration of HEX and diverse amounts of silver ions and inversely, for a fixed concentration of silver ions and different amounts of HEX. The same ratio of concentrations of HEX to silver was applied as in previous experiments (Fig. 5).

The results of investigations, presented in Fig. 6a, revealed that silver ions in the presence of HEX significantly induced cell membrane damage. The LDH release determined at HEX concentration of 120 mg L^{-1} was equal to 42% and 60% of control in the case of U-937 and HL-60 cells, respectively. It is worth emphasizing that it was ca. 20% higher than this observed for pure HEX. Moreover, in the case of HL-60 cells treated by the mixture of HEX with silver ions of concentration 32 mg L^{-1}, the LDH release was ca. 50% higher than this recorded for the silver solution of the same concentration (Fig. 3c).

Increasing concentration of HEX in solutions of silver ions of concentration of 4 mg L^{-1} (Fig. 6b) slightly

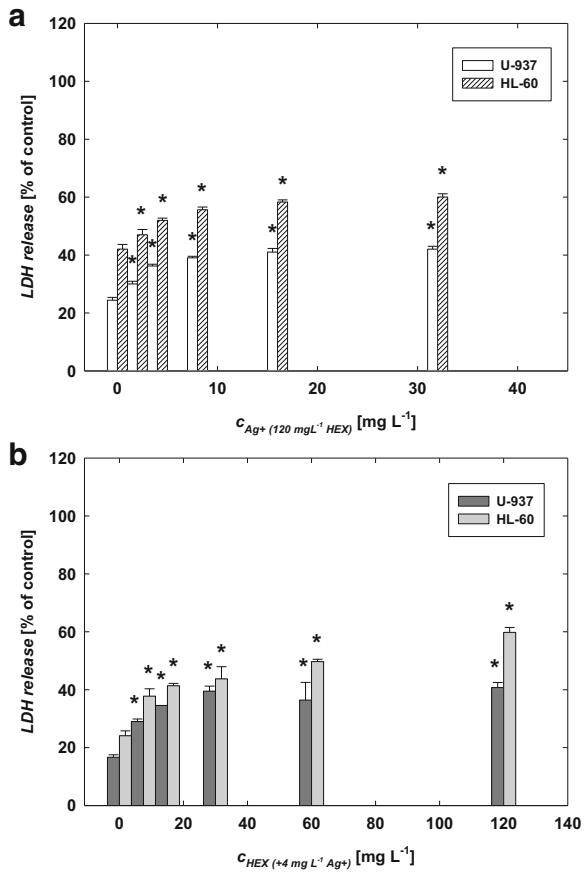

Fig. 6 Membrane damage indicated via LDH release after the cell treatment with (**a**) Ag^+ in the presence of HEX of concentration of 120 mg L^{-1}, (**b**) HEX in the presence of Ag^+ of concentration of 4 mg L^{-1}. (*) Statistically significant differences ($p < 0.05$) compared to controls

amplified the LDH release from U-937 and HL-60 cells. The highest enhancement of LDH secretion in comparison to the pure silver nitrate solution was found for HEX concentration of 120 mg L^{-1}. However, the mixtures of various concentration of HEX with silver ions (Fig. 6b) induced noticeably lower cell membrane damage than the mixtures with CITAgNPs (Fig. 5b).

SOD activity after the cell treatment with HEXAgNPs

Having regard to HEXAgNPs and HEX can generate strong oxidative stress in the cells (Fig. 4), the dependence of superoxide dismutase activity (SOD) on the HEXAgNP concentration was evaluated. The results of the experiments showed in Fig. 7 revealed that the activity of this antioxidant enzyme significantly decreased with the concentration of HEXAgNPs. For example, at a concentration of 2 mg L^{-1}, the SOD activity attained a value of 0.067 and 0.072 U/mg^{-1} of proteins for U-937 and HL-60 cells, respectively. On the other hand, the 18-fold increase of HEXAgNP concentration induced the reduction of SOD activity to 0.038 and 0.031 U/mg^{-1} of proteins for U-937 and HL-60 cells.

Discussion

In the literature cytotoxicity of AgNPs is widely investigated considering their size, shape, oxidative state, and surface properties (de Lima et al. 2012; Foldbjerg and Autrup 2013). In order to determine the possible mechanisms of AgNP activity, cellular response on AgNP

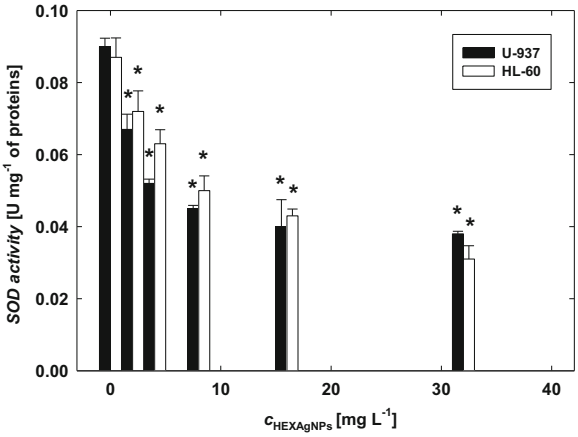

Fig. 7 SOD activity in the cells treated by HEXAgNPs. (*) Statistically significant differences ($p < 0.05$) compared with controls

treatment is assessed multi-directionally although one can notice that main attention is focused on the determination of oxidative stress, induction of inflammation, and changes in mitochondrial metabolism (de Lima et al. 2012). However, before AgNPs begin to stimulate a whole cascade of changes and cell processes, firstly they have to penetrate inside cells through their membranes. It was well-documented that penetration and uptake of AgNPs strongly depend on their size (Carlson et al. 2008). Nevertheless, the AgNP surface charge and chemical structure of coating layers also affect the interactions with cell membranes.

Having regard to the above, these studies were devoted to the impact of AgNP and their stabilizers on membrane damage causing cell death. The membrane integrity of U-937 and HL-60 cells was investigated using the LDH assay. Since negatively charged AgNPs are more often synthesized and applied in many branches of science and industry, two types of such nanoparticles, which were characterized by similar size distribution, average size, and ion release profile (Table 1), were used in these studies. HEXAgNPs were stabilized by sodium hexametaphosphate (HEX) which is a known food-grade permeabilizer. CITAgNPs, stabilized by trisodium citrate, were reference system similarly as silver ions delivered in the form of silver nitrate.

It was found that HEXAgNPs induced meaningful cell membrane damage in both cell lines. The cell viability decreased significantly with an increase of HEXAgNP concentration due to loss of membrane integrity (Fig. 3a) and disruption in mitochondrial activity (Supporting materials, Fig. 6S). Interestingly the LDH release induced by HEXAgNPs was higher than those determined for silver ions of the same concentration (Fig. 3c). Moreover, the profile of LDH leakage dependent on AgNPs-dose found for HEXAgNPs was slightly lower than this described by Avalos et al. (2014) for HL-60 cells treated by PVP and PEI-coated AgNPs of an average size of 4.7 ± 1 nm. Generally, Avalos et al. (2014) showed that LDH release in HepG2 and HL-60 cells increased significantly with the concentration and size reduction of AgNPs although the authors did not mention about the surface charge of investigated nanoparticles. An opposite effect was determined by Kim et al. (2012) for MC3T3 and PC1 cells treated by AgNPs of various sizes. The results of studies showed that LDH activity was significantly higher for larger AgNPs (100 nm) when compared to smaller sized nanoparticles (10–50 nm) (Kim et al. 2012). Nevertheless, in

this report, it was not given any information about the surface properties of the AgNPs.

Gliga et al. (2014) studied the size-dependent influence of uncoated, PVP and citrate-stabilized AgNPs on human lung cells and showed that after 24 h of treatment, the smallest nanoparticles but in the highest dose (50 mg L^{-1}) induced significant toxicity towards the cells. Moreover, none of the larger sized AgNPs alerted the cell viability. Hence, these outcomes were consistent with the results obtained by Avalos et al. (2014).

Schlinkert with coworkers (Schlinkert et al. 2015) were focused on the influence of surface properties of 7–10 nm AgNPs and AuNPs on their toxicity towards A549, BEAS-2B and primary lung epithelial cells (NHBE). The authors tested the biological activity of negatively charged citrate-stabilized nanoparticles and positively charged nanoparticles coated by chitosan. Despite the fact that stabilizers did not induce any effect on the viability and membrane integrity of the cells, it was found that positively charged nanoparticles (zeta potential above +60 mV) were highly harmful to the cells. The highest cell membrane impairment, detected via LDH release, was found for both types of the chitosan-stabilized nanoparticles. It was also noticed that the LDH leakage increased with chitosan loading.

The results of Schlinkert et al. (2015) are consistent with the findings obtained for CITAgNPs in the presence of HEX. As can be seen in Fig. 5b, the LDH release also increased with the concentration of HEX in the CITAgNP suspension. The highest differences in the cell membrane integrity, in comparison to pure CITAgNPs, were found for the highest concentration of HEX. It is worth mentioning that Schlinkert et al. (2015) postulated that the toxicity of investigated AgNPs and AuNPs was related to their surface charge. They concluded that AuNPs, which have been shown to be inert and often non-cytotoxic, can become toxic upon coating with certain charged molecules. CITAgNPs also became more toxic in the presence of HEX despite their zeta potential was highly (Fig. 2b) negative, even though in the presence of HEX (Supporting materials, Fig. 5S). Herein, one can speculate that HEXAgNPs were more toxic towards U-937 and HL-60 cells because their zeta potential was higher than the zeta potential of CITAgNPs (Fig. 2b). On the other hand, in our previous report (Barbasz et al. 2017), it was shown that the induction of LDH release in U-937 cells was lower in the case of positively charged cysteamine-stabilized AgNPs than in the case of negatively charged CITAgNPs. However, the reduction of HL-60 viability, determined in LDH assay, was comparable for these two types of AgNPs (Barbasz et al. 2017).

Previously described positively charged cysteine-stabilized AgNPs, characterized by comparable size distribution as the nanoparticles investigated in this work, also exhibited lower impact on the viability of U-937 and HL-60 cells (Oćwieja et al. 2017) than HEXAgNPs and CITAgNPs in the presence of HEX (Fig. 3a and Fig. 5a). Based on these findings one can hypothesize that not nanoparticle charge but stabilizers coating them play a pivotal role in mechanisms of their toxicity. Nevertheless, it is important to bear in mind that more often thanks to the chemical reactions which take place with the participation of the stabilizers (e.g., protonation), the metal nanoparticles are charged (Oćwieja et al. 2017).

It is worth emphasizing that in these studies, as well as in the work of Schlinkert et al. (2015), the enhancement of AgNP toxicity resulted from the fact that chitosan and HEX are biologically active substances (Kumar-Krishnan et al. 2015; Post et al. 1963). Although, chitosan is considered as nontoxic, some literature studies documented its toxicity towards human lymphoblastic leukemia (CCRF-CEM), human embryonic lung cells (L132), and murine melanoma cells (B16F10) (Kean and Thanou 2010). From one side one can suspect that maybe some cell lines, such as lung epithelial cells investigated by Schlinkert et al. (2015) and L132 cells studied by Richardson et al. (1999), are more sensitive to chitosan. Nevertheless, the hypothesis of Kean and Thanou (2010) related to the inappropriate conditions to cell viability determinations arising from chitosan solution preparation which contained other chemical substances can be also correct.

In the case of the studies described in this report, it was found that the applications of pure solutions of HEX influenced also the viability of the cells (Fig. 3d). Moreover, HL-60 cells were more sensitive to HEX than U-937 cells which were discovered via LDH (Fig. 3d) and MDA (Fig. 4b) assays. The same tendency was noticed for CITAgNPs mixed with HEX of concentration 120 mg L^{-1} (Fig. 5a) although the differences in the LDH release were lower in the case of pure HEX (Fig. 3d). It is worth mentioning that differences in the cell sensitivity to toxic agents can be directly related to significant differences in the cell membrane structures. Previously Schafer and Buettner (1999) hypothesized that due to the fact that cell lines can have different

content of polyunsaturated fatty acids (PUFA), the cellular response on the exposition to singlet oxygen will be different. The conducted results revealed that the greater the lipid content of the cell line, the less susceptible they are to membrane damage. Moreover, the authors observed that the greater the protein content of cells the more they were protected against membrane damage induced by Photofrin photosensitization. The authors showed that in the case of U-937 cells the total lipid content is 2.5-fold higher than for HL-60. Based on these studies, we assumed that U-937 cells are more resistant to the action of the AgNPs and HEX because they possess greater lipid content in the membranes than HL-60 cells.

At a stable concentration of CITAgNPs and for various concentrations of HEX (Fig. 5b), the differences between the LDH secretion determined for HL-60 and U-937 cells disappeared, similarly as in the case of mixtures of silver ions with diverse concentrations of HEX (Fig. 6b). Independently on the mixture composition (AgNPs or silver ions with HEX), the LDH release was higher than this one found for the pure solution of HEX, silver ions, or CITAgNPs. Based on these outcomes, it was possible to confirm the synergism between silver and HEX.

It was noticed that at a constant concentration of CITAgNPs (Fig. 5b) and silver ions (Fig. 6b), the LDH secretion did not grow significantly with HEX concentration. On the other hand, at HEX concentration of 120 mg L^{-1} the increase of CITAgNPs (Fig. 5a) or silver ions (Fig. 6a) noticeably enhanced LDH secretion. Therefore, it was deduced that the toxicity of the mixtures is mainly induced by silver.

It seems plausible that at low concentration HEX facilitates only the penetration of silver inside the cells. Therefore the effects observed at the given concentration of CITAgNPs and silver ions in the mixtures are slightly higher than these ones determined for pure suspension (Fig. 3b) and silver ions (Fig. 3c). Since pure HEX at high concentration induces cell death via the disruption in the cell membrane (Fig. 3d), it was found that the mixtures of HEX of concentration of 120 mg L^{-1} and an increasing amount of silver significantly induced LDH to release in comparison with pure HEX and silver solutions. HEX is toxic at higher concentrations for the cells and causes oxidative stress (Fig. 4b) as well as a decrease in the mitochondrial activity which was confirmed by MTT assay (Supporting materials, Fig. 6S).

Interestingly, it was observed that at the mitochondrial level the toxicity of HEXAgNPs and silver ions was comparable (Supporting materials, Fig. 6S). At a concentration of 8 mg L^{-1}, both forms of silver totally deactivated the cells. Otherwise, the same concentration of CITAgNPs and HEX did not disrupt the cell viability significantly.

Owing to the induction of oxidative stress by HEX and HEXAgNPs, the cell membrane damage was generated also by lipid peroxidation (Fig. 4). The activity of SOD was strongly inhibited by HEXAgNPs (Fig. 7). It is worth recalling that, at a low concentration of toxic factors, cells activate available cascades of defense systems in order to prevent their total damages. The increase of reactive oxygen species (ROS) causing oxidative stresses induces secretion of antioxidant enzymes, such as SOD, which should eliminate ROS. However, when the toxic factor is strong enough, it can destroy not only antioxidant enzymes but also whole prevention systems. Therefore, based on the outcomes related to SOD activity (Fig. 7) one can state that HEXAgNPs were much more toxic than CITAgNPs. It is worth adding that the decrease in SOD activity was also observed by Avalos et al. (2014) in the case of hepatoma and leukemia cells (HepG2 and HL-60 cells) treated by PVP and PEI-coated AgNPs of an average size of 4.7 ± 1 nm and 42 ± 9 nm.

Conclusions

The selection of the stabilizing agent of AgNPs is significant for their interaction with the cell membrane and their total biological activity. Sodium hexametaphosphate (HEX), potentially considered as nontoxic, enhances cytotoxicity of HEXAgNPs towards U-937 and HL-60 when it is applied as nanoparticle stabilizer. Nevertheless, the addition of HEX to citrate-stabilized AgNPs (CITAgNPs) and silver ions also improved their toxicity. Despite permeabilizing properties, at high concentration HEX can induce strong oxidative stress in the cells which leads to membrane lipid peroxidation and degradation of antioxidant enzymes. Though the intercellular response on the treatment with silver ions and HEXAgNPs was comparable on the mitochondrial level, the mechanisms of interaction of both forms of silver with cell membranes seem to be different. The increased secretion of LDH after the treatment with HEXAgNPs or CITAgNPs in the

presence of HEX in comparison to silver ions indicates that some geometric factor related to the size of active substance play important role in their toxicity.

On the one hand, the combinations of AgNPs and silver ions with HEX can find a broad range of biological and medical applications. Nevertheless, one can remember that HEXAgNPs do not possess target receptors towards only leukemia cells. HEXAgNPs do not exhibit selectivity towards normal and tumor cells, therefore more extensive studies are needed in order to fully understand the biological activity of compositions of silver and sodium hexametaphosphate. On the other hand, considering widespread of HEX in food and consumer products and still growing applications of AgNPs in common consumer goods one should remember that despite they are used separately, they can interact with each other in the environment inducing uncontrolled effects in living organisms.

Acknowledgments The authors are also grateful to Doctor Dorota Duraczyńska and Doctor Elżbieta Bielańska for taking imaging with the use of TEM.

Funding information This work was financially supported by the Polish Ministry of Science and Higher Education (MNiSW) under Iuventus Plus No. IP 2015055974 project. The authors would like to thank Stanisław Walas from the Jagiellonian University for the AAS measurements which were conducted using apparatus purchased, thanks to the financial support of the European Regional Development Fund in the framework of the Polish Innovation Economy Operational Program (contract no. POIG.02.01.00-12-023/0).

Compliance with ethical standards

Conflict of interest The authors declare that they have no conflict of interest.

References

Abbaszadegan A, Ghahramani Y, Gholami A, Hemmateenejad B, Dorostkar S, Nabavizadeh M, Sharghi H (2015) The effect of charge at the surface of silver nanoparticles on antimicrobial activity against gram-positive and gram-negative bacteria: a preliminary study. J Nanomater 16:53–58. https://doi.org/10.1155/2015/720654

Adamczyk Z, Kujda M, Oćwieja M (2016) Polish patent application P.401528

Ahamed M, Karns M, Goodson M, Rowe J, Hussain SM, Schlager JJ, Hong Y (2008) DNA damage response to different surface chemistry of silver nanoparticles in mammalian cells. Toxicol Appl Pharmacol 233:404–410. https://doi.org/10.1016/j.taap.2008.09.015

Ávalos Fúnez A, Isabel Haza A, Mateo D, Morales P (2013) In vitro evaluation of silver nanoparticles on human tumoral and normal cells. Toxicol Mech Methods 23:153–160. https://doi.org/10.3109/15376516.2012.762981

Avalos A, Haza AI, Mateo D, Morales P (2014) Cytotoxicity and ROS production of manufactured silver nanoparticles of different sizes in hepatoma and leukemia cells. J Apl Toxicol 34:413–423. https://doi.org/10.1002/jat.2957

Bae WJ, Jue SS, Kim SY, Moon JH, Kim EC (2015) Effects of sodium tri-and hexametaphosphate on proliferation, differentiation, and angiogenic potential of human dental pulp cells. J Endod 41:896–902. https://doi.org/10.1016/j.joen.2015.01.038

Barbasz A, Oćwieja M, Roman M (2017) Toxicity of silver nanoparticles towards tumoral human cell lines U-937 and HL-60. Colloids Surf B: Biointerfaces 156:397–404. https://doi.org/10.1016/j.colsurfb.2017.05.027

Cao H (2017) Silver nanoparticles for antibacterial devices: biocompatibility and toxicity. CRC Press. Chapter 3 synergistic antimicrobial activity of silver and chitosan. P.55, Sulbha K. Sharma, G. Kharkwal, Ying-Ying Huang, Michael R, Hamblin

Carlson C, Hussain SM, Schrand AM, Braydich-Stolle L, Hess KL, Jones RL, Schlager JJ (2008) Unique cellular interaction of silver nanoparticles: size-dependent generation of reactive oxygen species. J Phys Chem B 112:13608–13619. https://doi.org/10.1021/jp712087m

Dalpasquale G, Delbem ACB, Pessan JP, Nunes G, Gorup LF, Neto FNS, Danelon M (2017) Effect of the addition of nanosized sodium hexametaphosphate to fluoride toothpastes on tooth demineralization: an in vitro study. Clin Oral Investig 21:1821–1827. https://doi.org/10.1007/s00784-017-2093-3

de Lima R, Seabra AB, Durán N (2012) Silver nanoparticles: a brief review of cytotoxicity and genotoxicity of chemically and biogenically synthesized nanoparticles. J Appl Toxicol 32:867–879. https://doi.org/10.1002/jat.2780

Ding HM, Ma YQ (2012) Role of physicochemical properties of coating ligands in receptor-mediated endocytosis of nanoparticles. Biomaterials 33:5798–5802. https://doi.org/10.1016/j.biomaterials.2012.04.055

Fayaz AM, Balaji K, Girilal M, Yadav R, Kalaichelvan PT, Venketesan R (2010) Biogenic synthesis of silver nanoparticles and their synergistic effect with antibiotics: a study against gram-positive and gram-negative bacteria.

Nanomedicine 6:103–109. https://doi.org/10.1016/j.nano.2009.04.006

Foldbjerg R, Autrup H (2013) Mechanisms of silver nanoparticle toxicity. Arch Med Res 5-15

Fröhlich E (2012) The role of surface charge in cellular uptake and cytotoxicity of medical nanoparticles. Int J Nanomedicine 7:5577. https://doi.org/10.2147/IJN.S36111

Gliga AR, Skoglund S, Wallinder IO, Fadeel B, Karlsson HL (2014) Size-dependent cytotoxicity of silver nanoparticles in human lung cells: the role of cellular uptake, agglomeration and Ag release. Part Fibre Toxicol 11:11. https://doi.org/10.1186/1743-8977-11-11

Guo D, Zhu L, Huang Z, Zhou H, Ge Y, Ma W, Zhao Y (2013) Anti-leukemia activity of PVP-coated silver nanoparticles via generation of reactive oxygen species and release of silver ions. Biomaterials 34:7884–7894. https://doi.org/10.1016/j.biomaterials.2013.07.015

Gupta A, Singh P, Shivakumara C (2010) Synthesis of BaSO4 nanoparticles by precipitation method using sodium hexametaphosphate as a stabilizer. Solid State Commun 150:386–388. https://doi.org/10.1016/j.ssc.2009.11.039

Helander IM, Mattila-Sandholm T (2000) Permeability barrier of the gram-negative bacterial outer membrane with special reference to nisin. Int J Food Microbiol 60:153–161. https://doi.org/10.1016/S0168-1605(00)00307-X

Huang L, Dai T, Xuan Y, Tegos GP, Hamblin MR (2011) Synergistic combination of chitosan acetate with nanoparticle silver as a topical antimicrobial: efficacy against bacterial burn infections. Antimicrob Agents Chemother 55:3432–3438. https://doi.org/10.1128/AAC.01803-10

Humphreys G, Lee GL, Percival SL, McBain AJ (2011) Combinatorial activities of ionic silver and sodium hexametaphosphate against microorganisms associated with chronic wounds. Antimicrob Agents Chemother 66:2556–2561. https://doi.org/10.1093/jac/dkr350

Hwang IS, Hwang JH, Choi H, Kim KJ, Lee DG (2012) Synergistic effects between silver nanoparticles and antibiotics and the mechanisms involved. J Med Microbiol 61:1719–1726. https://doi.org/10.1099/jmm.0.047100-0

Jiang J, Oberdörster G, Biswas P (2009) Characterization of size, surface charge, and agglomeration state of nanoparticle dispersions for toxicological studies. J Nanopart Res 11:77–89. https://doi.org/10.1007/s11051-008-9446-4

Kaba SI, Egorova EM (2015) In vitro studies of the toxic effects of silver nanoparticles on HeLa and U937 cells. Nanotechnol Sci Appl 8:19. https://doi.org/10.2147/NSA.S78134

Kean T, Thanou M (2010) Biodegradation, biodistribution and toxicity of chitosan. Adv Drug Deliv Res 62:3–11. https://doi.org/10.1016/j.addr.2009.09.004

Kim TH, Kim M, Park HS, Shin US, Gong MS, Kim HW (2012) Size-dependent cellular toxicity of silver nanoparticles. J Biomed Mater Res A 100:1033–1043. https://doi.org/10.1002/jbm.a.34053

Kittler S, Greulich C, Diendorf J, Koller M, Epple M (2010) Toxicity of silver nanoparticles increases during storage because of slow dissolution under release of silver ions. Chem Mater 22:4548–4554. https://doi.org/10.1021/cm100023p

Kujda M, Ościeja M, Adamczyk Z, Bocheńska O, Braś G, Kozik A, Bielańska E, Barbasz J (2015) Charge stabilized silver nanoparticles applied as antibacterial agents. J Nanosci Nanotechnol 15:3574–3583. https://doi.org/10.1166/jnn.2015.9727

Kumar-Krishnan S, Prokhorov E, Hernández-Iturriaga M, Mota-Morales JD, Vázquez-Lepe M, Kovalenko Y, Luna-Bárcenas G (2015) Chitosan/silver nanocomposites: synergistic antibacterial action of silver nanoparticles and silver ions. Eur Polym J 67:242–251. https://doi.org/10.1016/j.eurpolymj.2015.03.066

Lanigan RS (2001) Final report on the safety assessment of sodium metaphosphate, sodium trimetaphosphate, and sodium hexametaphosphate. Int J Toxicol 20:75–89. https://doi.org/10.1080/10915810152630756

Le Ouay B, Stellacci F (2015) Antibacterial activity of silver nanoparticles: a surface science insight. Nanotoday 10:339–354. https://doi.org/10.1016/j.nantod.2015.04.002

Li P, Li J, Wu C, Wu Q, Li J (2005) Synergistic antibacterial effects of β-lactam antibiotic combined with silver nanoparticles. Nanotechnology 16:1912–1917. https://doi.org/10.1088/0957-4484/16/082

Li Z, Wang Y, Yu Q (2010) Significant parameters in the optimization of synthesis of silver nanoparticles by chemical reduction method. J Mater Eng Perform 19:252–256. https://doi.org/10.1007/s11665-009-9486-7

Li Y, Zhang W, Niu J, Chen Y (2013) Surface-coating-dependent dissolution, aggregation, and reactive oxygen species (ROS) generation of silver nanoparticles under different irradiation conditions. Environ Sci Technol 47:10293–10301. https://doi.org/10.1021/es400945v

Liu W, Wu Y, Wang C, Li HC, Wang T, Liao CY, Jiang GB (2010) Impact of silver nanoparticles on human cells: effect of particle size. Nanotoxicology 4:319–330. https://doi.org/10.3109/17435390.2010.483745

Lu Z, Rong K, Li J, Yang H, Chen R (2013) Size-dependent antibacterial activities of silver nanoparticles against oral anaerobic pathogenic bacteria. J Mater Sci Mater Med 24:1465–1471. https://doi.org/10.1007/s10856-013-4894-5

Mendes-Gouvêa CC, do Amaral JG, Fernandes RA, Fernandes GL, Gorup LF, Camargo ER, Barbosa DB (2018) Sodium trimetaphosphate and hexametaphosphate impregnated with silver nanoparticles: characteristics and antimicrobial efficacy. Biofouling 34:299–308. https://doi.org/10.1080/08927914.2018.1437146

Morga M, Adamczyk Z (2013) Monolayers of cationic polyelectrolytes on mica: Electrokinetic studies. J Colloid Interface Sci 407:196–204. https://doi.org/10.1016/j.jcis.2013.05.069

Ościeja M, Barbasz A, Walas S, Roman M, Paluszkiewicz C (2017) Physicochemical properties and cytotoxicity of cysteine-functionalized silver nanoparticles. Colloids Surf B: Biointerfaces 160:429–437. https://doi.org/10.1016/j.colsurfb.2017.09.042

Pal S, Tak YK, Song JM (2007) Does the antibacterial activity of silver nanoparticles depend on the shape of the nanoparticle? A study of the gram-negative bacterium Escherichia coli. Appl Environ Microbiol 73:1712–1720. https://doi.org/10.1128/AEM.02218-06

Parab HJ, Huang JH, Lai TC, Jan YH, Liu RS, Wang JL, Chuang SY (2011) Biocompatible transferrin-conjugated sodium hexametaphosphate-stabilized gold nanoparticles: synthesis, characterization, cytotoxicity and cellular uptake. Nanotechnology 22:395706. https://doi.org/10.1088/0957-4484/22/39/395706

Pokhrel LR, Dubey B, Scheuerman PR (2013) Impacts of select organic ligands on the colloidal stability, dissolution dynamics, and toxicity of silver nanoparticles. Environ Sci Technol 47:12877–12885. https://doi.org/10.1021/es403462j

Post FJ, Krishnamurty GB, Flanagan MD (1963) Influence of sodium hexametaphosphate on selected bacteria. Appl Environ Microbiol 11:430–435

Potara M, Jakab E, Damert A, Popescu O, Canpean V, Astilean S (2011) Synergistic antibacterial activity of chitosan–silver nanocomposites on Staphylococcus aureus. Nanotechnology 22:135101. https://doi.org/10.1088/0957-4484/22/13/135101

Richardson SW, Kolbe HJ, Duncan R (1999) Potential of low molecular mass chitosan as a DNA delivery system: biocompatibility, body distribution and ability to complex and protect DNA. Int J Pharm 178:231–243. https://doi.org/10.1016/S0378-5173(98)00378-0

Ruden S, Hilpert K, Berditsch M, Wadhwani P, Ulrich AS (2009) Synergistic interaction between silver nanoparticles and membrane-permeabilizing antimicrobial peptides. Antimicrob Agents Chemother 53:3538–3540. https://doi.org/10.1128/AAC.01106-08

Schafer FQ, Buettner GR (1999) Single oxygen toxicity is cell line-dependent: a study of lipid peroxidation in nine leukemia cell lines. Photochem Photobiol 70:858–867. https://doi.org/10.1111/j.1751-1097.1999.tb08294.x

Schlinkert P, Casals E, Boyles M, Tischler U, Hornig E, Tran N, Puntes V (2015) The oxidative potential of differently charged silver and gold nanoparticles on three human lung epithelial cell types. J Nanobiotechnol 13:1. https://doi.org/10.1186/s12951-014-0062-4

Suresh AK, Pelletier DA, Wang W, Morrell-Falvey JL, Gu B, Doktycz MJ (2012) Cytotoxicity induced by engineered silver nanocrystallites is dependent on surface coatings and cell types. Langmuir 28:2727–2735. https://doi.org/10.1021/la2042058

Vaara M (1992) Agents that increase the permeability of the outer membrane. Microbiol Mol Biol Rev 56:395–411

Vaara M, Jaakkola (1989) Sodium hexametaphosphate sensitizes Pseudomonas aeruginosa, several other species of Pseudomonas, and Escherichia coli to hydrophobic drugs. Antimcrob Agents Chemother 33:1741–1747. https://doi.org/10.1128/AAC.33.10.1741

Warad HC, Ghosh SC, Hemtanon B, Thanachayanont C, Dutta J (2005) Luminescent nanoparticles of Mn doped ZnS passivated with sodium hexametaphosphate. Sci Technol Adv Mater 6:296–301. https://doi.org/10.1016/j.stam.2005.03.006

Zhang S, Li J, Lykotrafitis G, Bao G, Suresh S (2009) Size-dependent endocytosis of nanoparticles. Adv Mater 21:419–424. https://doi.org/10.1002/adma.200801393

Zhang W, Yao Y, Sullivan N, Chen Y (2011) Modeling the primary size effects of citrate-coated silver nanoparticles on their ion release kinetics. Environ Sci Technol 45:4422–4428. https://doi.org/10.1021/es104205a